A Journal of the Gesellschaft Deutscher Chemiker

Angewandte International Edition Chemie

GDCh

www.angewandte.org

Accepted Article

Title: 4,5,9,10-Pyrene Diimides: A New Family of Aromatic Diimides Exhibiting High Electron Mobility and Two-Photon Excited Emission

Authors: Ze-Hua Wu, Zhuo-Ting Huang, Rui-Xue Guo, Chun-Lin Sun, Li-Chuan Chen, Bing Sun, Zi-Fa Shi, Xiangfeng Shao, Hanying Li, and Hao-Li Zhang

To be cited as: *Angew. Chem. Int. Ed.* 10.1002/anie.201707529
Angew. Chem. 10.1002/ange.201707529

Link to VoR: http://dx.doi.org/10.1002/anie.201707529
http://dx.doi.org/10.1002/ange.201707529

WILEY-VCH

10.1002/anie.201707529

WILEY-VCH

4,5,9,10-Pyrene Diimides: A New Family of Aromatic Diimides Exhibiting High Electron Mobility and Two-Photon Excited Emission

Ze-Hua Wu[a], Zhuo-Ting Huang[c], Rui-Xue Guo[a], Chun-Lin Sun[a], Li-Chuan Chen[a], Bing Sun[a], Zi-Fa Shi[a], Xiangfeng Shao[a], Hanying Li*[c] and Hao-Li Zhang*[a], [b]

Abstract: Design and synthesis of high performance n-type organic semiconductors are important for the development of future organic optoelectronics. Herein, we report the facile synthetic routes to reach the K-region of pyrene and produce 4,5,9,10-pyrene diimide (**PyDI**) derivatives. The **PyDI** derivatives exhibited efficient electron transport properties with the highest electron mobility up to 3.08 $cm^2V^{-1}s^{-1}$. Besides, the tert-butyl substituted compounds (**t-PyDI**) also showed good one and two photon excited fluorescence properties. The **PyDI** derivatives are new family of aromatic diimides that may exhibit both high electron mobility and good light emitting properties, making them excellent candidates for future optoelectronics.

Organic semiconductors have attracted considerable academic and commercial interest in recent years for their potential in constructing low cost, stretchable[1] and solution-processed large-area[2] electronics. In general, the development of n-type organic semiconductors largely lagged behind the p-type counterparts, which has limited the development of practical organic electronics.[3] Large numbers of n-type semiconductors have been reported in the last few years, which mostly based on electron deficient frameworks, like perylene diimide (PDI),[4] naphthalene diimide (NDI),[5] diketopyrrolopyrrole (DPP)[6] and heteroacenes[7] etc. However, the number of high performance n-type organic semiconductors is still very limited.[8] Therefore, developing new electron deficient frameworks for n-type organic semiconductors is of great importance.

Aromatic diimides are among the most important classes of n-type organic materials. Classical semiconductors like NDI and PDI (Fig. 1) derivatives have found wide applications in optoelectronics. After decades efforts of structural optimization, the highest electron mobilities from NDI and PDI based small molecules have reached 8.6[9] and 10.8[10] $cm^2V^{-1}s^{-1}$, respectively. Significant efforts have been made to design new diimide skeleton, including pyromellitic diimides,[11] anthracene diimide (ADI)[12] and 1,2,5,6-naphthalene diimide[13]. However, the electron motilities of these new diimides have not exceeded 1 $cm^2V^{-1}s^{-1}$.

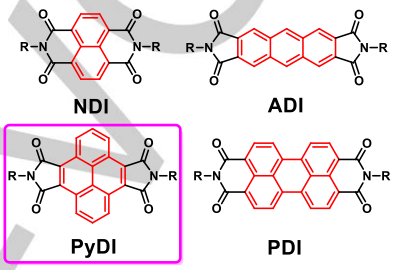

Figure 1. Comparison between the structures of **PyDI** and other representative linear aromatic diimides, including NDI, ADI and PDI.

To date, nearly all the small acenes have been used as core for construction of aromatic diimides, except pyrene. Pyrene consists of four-ring-fused planar electron enriched skeleton, which is well known for high photoluminescence efficiency.[14] Only until very recently, researchers are able to synthesize pyrene-based diimide. Pei and colleagues described the synthesis of 1,2,6,7-pyrene diimde, but no charge transport property was reported.[15] Yu's group has employed 4,5,9,10-pyrene diimide unit in solar cell materials which exhibited the highest electron mobility of 8×10^{-4} $cm^2V^{-1}s^{-1}$ in blend.[16] Herein, we report the first class of pyrene-diimide small molecules exhibiting excellent charge transport capability and attractive optical properties. By using two different synthetic routes, we obtained a series of axisymmetric 4,5,9,10-pyrene diimide (**PyDI**) derivatives. Electron mobility of **PyDI** derivatives in field effect transistor reached 3.08 $cm^2V^{-1}s^{-1}$, making them one of the best classes of diimide-based organic semiconductors.

Previous researches [13, 17] have revealed that axisymmetric diimides (typically NDI and PDI) are generally preferred due to desirable intramolecular charge distribution and π-π overlap in crystals. The ideal positions for constructing axisymmetric pyrene diimide are the 4,5,9,10-positions (K-region) of pyrene. However, the main obstacle to the synthesis is that the electrophilic substitution of pyrene preferentially takes place at the 1,3,6,8-positions, so that accessing the K-region is difficult.

To achieve ideal regioselectivity, we developed two feasible strategies to synthesize the 4,5,9,10-pyrene diimides (**PyDI**), which are illustrated in **Scheme 1**. Route 1 is inspired by Yu's work[16], which uses 1,2,3,6,7,8-hexahydropyrene as the starting material and converts the core to pyrene after introducing diimdes. The main problem with this route is that the intermediate compounds **1**-**4** are nearly insoluble in most

[a] Z. H. Wu, R. X. Guo, Dr. C. L. Sun, L. C. Chen, B. Sun, Prof. Z. F. Shi, Prof. X. F. Shao, and Prof. H. L. Zhang
State Key Laboratory of Applied Organic Chemistry
Key Laboratory of Special Function Materials and Structure Design
College of Chemistry and Chemical Engineering
Lanzhou University, Lanzhou 730000 (P. R. China)
E-mail: haoli.zhang@lzu.edu.cn
[b] Prof. H. L. Zhang
Tianjin Key Laboratory of Molecular Optoelectronic Sciences
Collaborative Innovation Center of Chemical Science and Engineering
Tianjin 300072 (P. R. China)
E-mail: haoli.zhang@lzu.edu.cn
[c] Ms. Z. T. Huang, Prof. H. Y. Li
State Key Laboratory of Silicon Materials
Key Laboratory of Macromolecule Synthesis and Functionalization
Department of Polymer Science and Engineering
Zhejiang University, Hangzhou 310027 (P. R. China)
E-mail: hanying_li@zju.edu.cn

Supporting information for this article is given via a link at the end of the document.

organic solvents, making the processing and characterization difficult. To overcome the solubility problem, we designed another synthetic route. Route 2 employs positional protective tert-butyl groups at the 2,7-positions of pyrene, so that the diimide units could be introduced to the desired 4,5,9,10 positions. This synthetic route affords 2,7-ditert-butyl-4,5,9,10-pyrene diimde (**t-PyDI**) in good yield. In the presence of tert-butyl groups, the intermediate compounds **5**-**9** and the product **t-PyDI** have excellent solubility in common organic solvents. Details of the synthesis along with the characterization data are available in the Supporting Information. In both routes, the alkyl chains on the nitrogen atoms can be easily varied by using different amines as reactants. In the following discussion, we will use the n-pentyl moiety substituted compounds, named as **C_5-PyDI** and **t-C_5-PyDI**, as the typical examples, while the properties of the other compounds are provided in the Supporting Information.

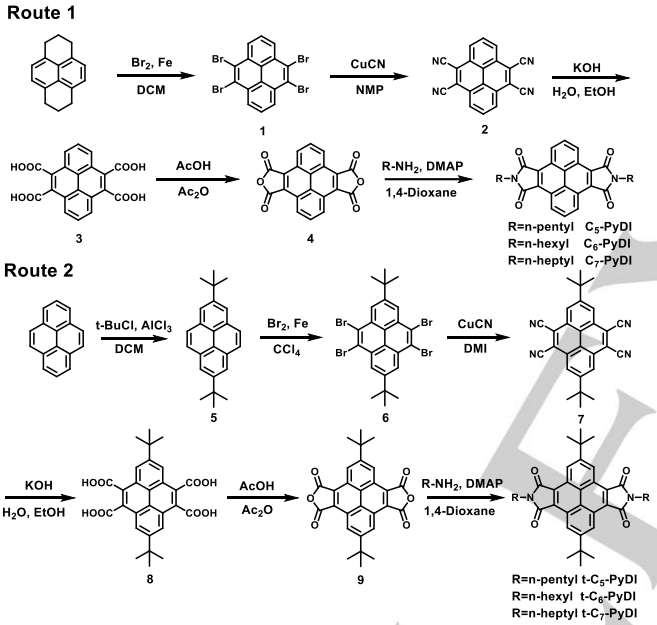

Scheme 1. Synthetic routes to **PyDI** and **t-PyDI**

The single crystal X-ray diffraction (XRD) (Fig. 2) shows that the **C_5-PyDI** crystalizes into triclinic system with P-1 space group, in which the molecule adopts a rigid and planar conformation with 1-D π-stacking motif. The closest planar distance of the nearest molecules is 3.414 Å indicating strong π-π interactions, which is favourable for charge transport. In contrast, the **t-C_5-PyDI** crystalizes into monoclinic system with P 2/c space group. In the crystals, the pyrene core of the **t-C_5-PyDI** is slightly twisted to compensate the steric hindrance of the tert-butyl moieties and to maximize the π-π interactions. As a result, the molecules pack into a lamellar motif with two neighbouring molecules forming a pair (Fig. 2f). In each pair, the nearest two molecules have large π-π overlap with the closest distance measured to be 3.165 Å. However, each pair is separated from the neighbouring pair by the n-pentyl chains and the closest distance between the adjacent pairs is around 7.349 Å. The large separation between the adjacent pairs may hinder charge transport, but such lamellar motif and twisted conformation could be beneficial for solid state light emission.[18]

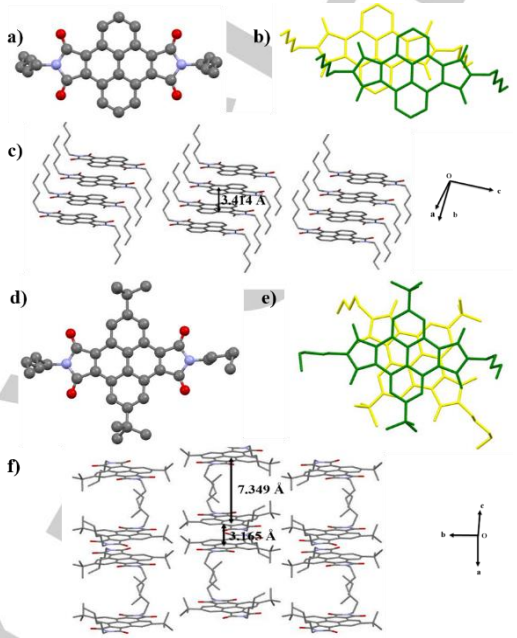

Figure 2. Single crystal structure (a), top view (b) and side view (c) of the crystal packing diagram of **C_5-PyDI**. Single crystal structure (d), top view (e) and side view (f) of the crystal packing diagram of **t-C_5-PyDI**. Hydrogen atoms are omitted for clarity.

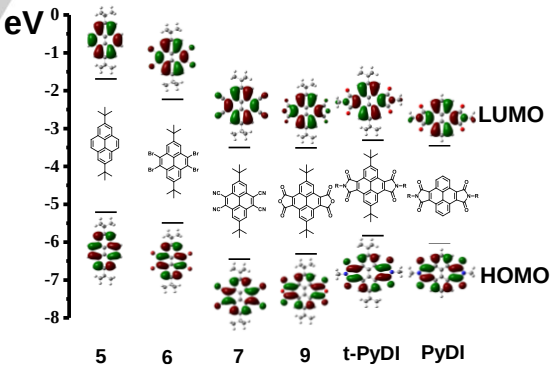

Figure 3. An illustration of the frontier molecular orbitals of the compounds **5**, **6**, **7**, **9**, **t-PyDI** and **PyDI**.

With the tert-butyl groups providing enough solubility, the change of electronic properties along the route 2 was readily followed by various spectroscopic and electrochemical characterizations in solutions. The UV-vis spectra and cyclic voltammetry curves of the compounds **5**, **6**, **7**, **9**, **t-C_5-PyDI** and **C_5-PyDI** are shown in Fig. S1 and S2. Table S1 summarizes the electronic properties of these compounds obtained from cyclic voltammetry and density functional theory (DFT) calculations using Gaussian [DFT/B3LYP/6-311+G(d,p)] package. Fig. 3

compares the energy levels and frontier molecular orbitals of these compounds. The LUMO energy levels are dramatically lowered from compounds **5** (-1.69 eV) to **7** (-3.50 eV) due to the introduction of electron withdrawing groups. Compared with the compound **9**, the LUMO energy level of **t-C$_5$-PyDI** raises slightly, which is attributed to electron donating effect of the lone pair electrons on the nitrogen. The HOMO and LUMO levels of **C$_5$-PyDI** decrease 0.23 eV and 0.14 eV, respectively, compared with **t-C$_5$-PyDI**, due to the hyper conjugation and electron donating effect of the tert-butyl groups. Fig. 3 clearly illustrates that by attaching different electron withdrawing groups, the energy levels of pyrene are systematically tuned.

We investigated the fluorescence properties of the **C$_5$-PyDI** and **t-C$_5$-PyDI** in both solution and solid states. In diluted solutions lower than 1×10^{-7} mol/L, the fluorescence quantum yield (FQY) of **C$_5$-PyDI** is 59.7%. The **t-C$_5$-PyDI** gives even higher fluorescence quantum yield of 79.5%. In solid state, the **C$_5$-PyDI** shows a total quench of the fluorescence due to strong intermolecular interaction in crystals.[19] In contrast, **t-C$_5$-PyDI** shows light yellow colour with a fluorescence quantum yield of 6.15% in solid.

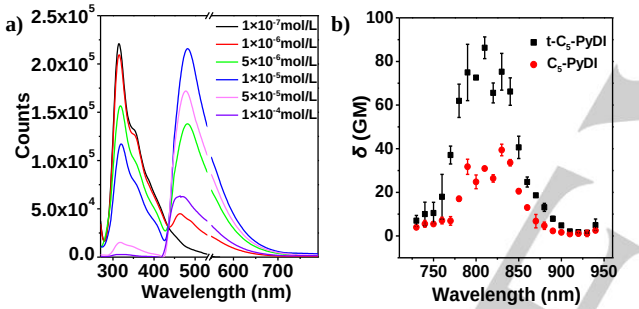

Figure 4. Emission spectra of **t-C$_5$-PyDI** in cyclohexane excited at 270 nm (The spectra are blanked in the range of 520-560 nm in order to remove the second order diffraction peak of excitation light) (a). Dispersion of two photon absorption cross section of **t-C$_5$-PyDI** and **C$_5$-PyDI** in chloroform (b).

The formation of pyrene excimer is an important phenomenon which can be used in designing fluorescent labelled probes and biosensors.[20] Recently, Pei[15] and Köhler[21] have reported formation of excimer in pyrene-based small molecules and polymers, respectively. The excimer formation of **t-C$_5$-PyDI** (Fig. 4a) in cyclohexane was studied by recording the emission spectra under different concentrations (**C$_5$-PyDI** was not studied due to poor solubility). In the low concentration of 1×10^{-7} mol/L, two structural fluorescence bands peaked at 307 and 352 nm emerges. When the concentration gradually increases to 1×10^{-6} mol/L, a new broad band appears at 480 nm. The unstructured emission band at 480 nm is attributed to the formation of excimer.[22] The emergence of the new band is accompanied by the decrease of the bands at low wavelength. Further increasing the concentration to 1×10^{-4} mol/L, the emission bands of monomer disappear, with an isostilbic point at 435 nm. Meanwhile, as the concentration increases, the integral area of the emission spectra decreases, indicative of lower FQY in high concentrations. For instance, when the concentration of **t-C$_5$-PyDI** changes from 1×10^{-7} mol/L to 1×10^{-4} mol/L in cyclohexane, the FQY reduces from 79.5% to 18.3%.

Two photon absorption (TPA) is a process where molecules can absorb two less energetic photons simultaneously. Fluorescent molecules with large TPA cross sections may provide enhanced light penetration, high spatial resolution and low specimen photo damage in imaging applications.[23] The dispersion of TPA cross section of **C$_5$-PyDI** and **t-C$_5$-PyDI** between 730 nm and 940 nm are shown in Fig. 4b. The maximum TPA cross section of **t-C$_5$-PyDI** and **C$_5$-PyDI** occur from 790 nm to 840 nm, which matches well with the optical window in biological tissue.[24] The highest TPA cross sections of **t-C$_5$-PyDI** and **C$_5$-PyDI** are 89.15 GM and 40.74 GM, respectively, which are sufficient for two photon fluorescence microscopy imaging applications.[25] In comparison, simple NDI and PDI have nearly no fluorescence and negligible TPA cross section in the near-infrared wavelength region.[26] The high TPA cross sections of **PyDI** derivatives are attributed to the highly emissive property and proper length of π system of the pyrene core.[25]

We found that the n-pentyl and n-hexyl chains appear to be of the appropriate length for solution processible materials. Shorter chains give poor solubility, while longer chains, like n-heptyl chain, induce poor crystallinity and hence very poor device performance (Fig. S9). Thus, we report herein organic field effect transistors (OFETs) fabricated based on the crystals of **C$_5$-PyDI**, **t-C$_5$-PyDI** and their n-hexyl substituted analogues **C$_6$-PyDI** and **t-C$_6$-PyDI**. Crystals were prepared by the method of droplet-pinned crystallization (DPC).[27] Details of device fabrication are described in the Supporting Information. The **t-C$_5$-PyDI** and **t-C$_6$-PyDI** formed narrow and short nano/microrod-like single crystals with many branches, and most of the crystals did not bridge across the channel between source and drain electrodes (S-D electrodes) (Fig. S9). While for **C$_5$-PyDI** and **C$_6$-PyDI** the crystal ribbons were much longer and wider and arranged on the substrate regularly (Fig. 5), favouring charge transport.[28]

The polarized-light micrograph (Fig. S12) and selected area electron diffraction (SAED) patterns (Fig. S13) of the **C$_5$-PyDI** and **C$_6$-PyDI** nano-ribbons support their single-crystalline nature. SAED patterns indicate that the molecular packing within the nano-ribbons of **C$_5$-PyDI** and **C$_6$-PyDI** are identical to those in the single crystal. Furthermore, the transmission electron microscopy (TEM) and SAED identify that [010] is the preferable growth direction of the crystal ribbons of **C$_5$-PyDI** and **C$_6$-PyDI**. The X-ray diffractions from the DPC films of **C$_5$-PyDI**, **C$_6$-PyDI** and **t-C$_5$-PyDI** are shown in Fig. S14. The XRD peaks of the films of **C$_5$-PyDI** and **C$_6$-PyDI** correspond to the (001) diffractions as derived from the single crystal structure. However, the XRD of **t-C$_5$-PyDI** shows a broad diffraction band around ~25 degree with low intensity, indicating poor-crystallinity.

Based on these aligned single crystals, FETs were constructed by depositing a layer of 70 nm Au as the source and drain electrodes in the bottom-gate and top-contact configuration.

The transfer and output characteristic curves of **t-C$_5$-PyDI**, **C$_5$-PyDI** and **C$_6$-PyDI** (Fig. S11) were tested in glove box. **t-C$_6$-PyDI** shows no mobility.

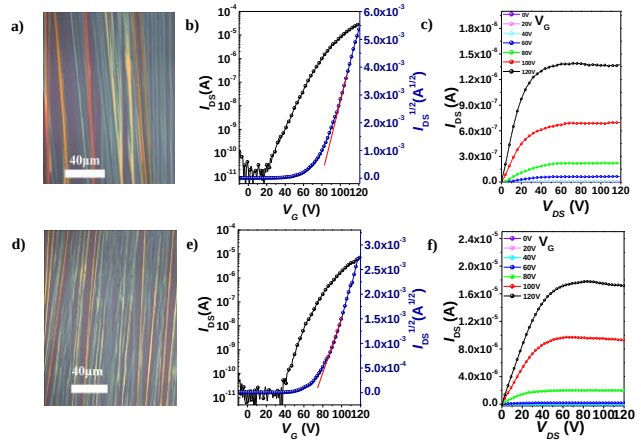

Figure 5. The optical microscopy (OM) image of the crystals (a), typical transfer (b) and output characteristics curves (c) of **C$_5$-PyDI**. The OM image of the crystals (d), typical transfer (e) and output characteristics curves (f) of **C$_6$-PyDI**. (Ag was used as electrode).

Table 1. OFET performance data for **t-C$_5$-PyDI**, **C$_5$-PyDI** and **C$_6$-PyDI** crystals.

Compound	S-D Electrode	Mobility [$cm^2V^{-1}s^{-1}$] [a]	on/off ratio	V_T (V)
t-C$_5$-PyDI	Au	2.51×10^{-4} ($8.72\times10^{-5}\pm0.91\times10^{-5}$)	$>10^3$	49-60
	Ag	-	-	-
C$_5$-PyDI	Au	0.46(0.19±0.13)	$>10^6$	43-50
	Ag	3.08(1.92±0.19)	$>10^6$	45-62
C$_6$-PyDI	Au	0.51(0.29±0.12)	$>10^6$	45-60
	Ag	2.36(2.05±0.17)	$>10^6$	49-68

[a] The values in the parentheses represent average mobility ± standard deviation.

The field effect mobility (μ) was calculated in the saturation regime with the equation: $I_{DS}=\mu C_0(W/2L)(V_G-V_T)^2$, where the I_{DS} is the current of S-D electrodes, μ is the field effect mobility, W and L are the width and length of the channel. The drop casted crystalline ribbons only partially covered the channel region. Therefore, the W and L were measured instead of using the channel dimensions of the shadow mask (Fig. S10). C_0 is the gate dielectric capacitance. The divinyltetramethyldisiloxane bis(benzocyclobutene) (BCB) covered SiO_2/Si substrates showed the capacitance of 1.1×10^{-8} F. V_G is the gate voltage and V_T is the threshold voltage. All the devices exhibited n-type behaviour. The highest electron transport mobility (μ_e) of **t-C$_5$-PyDI**, **C$_5$-PyDI** and **C$_6$-PyDI** were 2.5×10^{-4} $cm^2V^{-1}s^{-1}$, 0.46 $cm^2V^{-1}s^{-1}$ and 0.51 $cm^2V^{-1}s^{-1}$, respectively. Together with the mobility, the on/off ratios and threshold voltage (V_T) are shown in Table 1, where each average value was obtained from more than 20 working devices on 8 different substrates. Further optimization was performed on the OFET devices of **C$_5$-PyDI** and **C$_6$-PyDI** using Ag electrodes, which has a lower work function than Au. The conditions of crystals' growth were maintained as above for comparison. When using Ag as the S-D electrodes, the highest μ_e of **C$_5$-PyDI** and **C$_6$-PyDI** increases to 3.08 $cm^2V^{-1}s^{-1}$ and 2.36 $cm^2V^{-1}s^{-1}$, respectively.

PyDI is the first class of pyrene diimide framework that enables efficient charge transport. The highest electron mobility of **C$_5$-PyDI** reached up to 3.08 $cm^2V^{-1}s^{-1}$, which has outperformed most of the reported diimides.[3b, 4-5, 11-13] Meanwhile, the **t-C$_5$-PyDI** molecules exhibited lower electron mobility but higher one and two photon excited fluorescence emission properties. This work illustrates that the **PyDI** framework can be an excellent platform for designing new n-type organic semiconductors with high electron mobility and good one and two photon excited light emitting properties. It is expected that further structural modification to the **PyDI** skeleton could give even higher performance. The **PyDI** semiconductor family may find more practical applications in the future optoelectronics.

Acknowledgements

This work is supported by the Ministry of Science and Technology of China (2017YFA0204903), National Natural Science Foundation of China (NSFC. 51525303, 21233001, 21572086, 51625304, 21522203), 111 Project. The authors thank beam line BL14B1 (Shanghai Synchrotron Radiation Facility) for providing the beam time.

Keywords: pyrene • diimide • organic semiconductors • two photon absorption • electron transport

[1] T. Someya, Z. Bao, G. G. Malliaras, *Nature* **2016**, *540*, 379-385.
[2] M. R. Niazi, R. Li, M. Abdelsamie, K. Zhao, D. H. Anjum, M. M. Payne, J. Anthony, D.-M. Smilgies, A. Amassian, *Adv. Funct. Mater.* **2016**, *26*, 2371-2378.
[3] a) H. Klauk, U. Zschieschang, J. Pflaum, M. Halik, *Nature* **2007**, *445*, 745-748; b) C. Wang, H. Dong, W. Hu, Y. Liu, D. Zhu, *Chem. Rev.* **2012**, *112*, 2208-2267.
[4] S. Chen, P. Slattum, C. Wang, L. Zang, *Chem. Rev.* **2015**, *115*, 11967-11998.
[5] M. A. Kobaisi, S. V. Bhosale, K. Latham, A. M. Raynor, S. V. Bhosale, *Chem. Rev.* **2016**, *116*, 11685-11796.
[6] J. Lee, A. R. Han, J. Kim, Y. Kim, J. H. Oh, C. Yang, *J. Am. Chem. Soc.* **2012**, *134*, 20713-20721.
[7] X. Xu, Y. Yao, B. Shan, X. Gu, D. Liu, J. Liu, J. Xu, N. Zhao, W. Hu, Q. Miao, *Adv. Mater.* **2016**, *28*, 5276-5283.
[8] G. Xue, J. Wu, C. Fan, S. Liu, Z. Huang, Y. Liu, B. Shan, H. L. Xin, Q. Miao, H. Chen, H. Li, *Mater. Horiz.* **2016**, *3*, 119-123.
[9] T. He, M. Stolte, C. Burschka, N. H. Hansen, T. Musiol, D. Kälblein, J. Pflaum, X. Tao, J. Brill, F. Würthner, *Nat. Commun.* **2015**, *6*, 5954.
[10] N. A. Minder, S. Ono, Z. Chen, A. Facchetti, A. F. Morpurgo, *Adv. Mater.* **2012**, *24*, 503-508.
[11] Q. Zheng, J. Huang, A. Sarjeant, H. E. Katz, *J. Am. Chem. Soc.* **2008**, *130*, 14410-14411.

[12] Z. Wang, C. Kim, A. Facchetti, T. J. Marks, *J. Am. Chem. Soc.* **2007**, *129*, 13362-13363.
[13] S.-c. Chen, Q. Zhang, Q. Zheng, C. Tang, C.-Z. Lu, *Chem. Commun.* **2012**, *48*, 1254-1256.
[14] T. M. Figueira-Duarte, K. Müellen, *Chem. Rev.* **2011**, *111*, 7260-7314.
[15] L. Zou, X.-Y. Wang, X.-X. Zhang, Y.-Z. Dai, Y.-D. Wu, J.-Y. Wang, J. Pei, *Chem. Commun.* **2015**, *51*, 12585-12588.
[16] D. Zhao, Q. Wu, Z. Cai, T. Zheng, W. Chen, J. Lu, L. Yu, *Chem. Mater.* **2016**, *28*, 1139-1146.
[17] X.-K. Chen, L.-Y. Zou, J.-F. Guo, A.-M. Ren, *J. Mater. Chem.* **2012**, *22*, 6471-6484.
[18] C.-L. Sun, J. Li, H.-W. Geng, H. Li, Y. Ai, Q. Wang, S.-L. Pan, H.-L. Zhang, *Chem. Asian J.* **2013**, *8*, 3091-3100.
[19] a) G. Chen, W. Li, T. Zhou, Q. Peng, D. Zhai, H. Li, W. Z. Yuan, Y. Zhang, B. Z. Tang, *Adv. Mater.* **2015**, *27*, 4496-4501; b) R. H. Friend, R. W. Gymer, A. B. Holmes, J. H. Burroughes, R. N. Marks, C. Taliani, D. D. C. Bradley, D. A. D. Santos, J. L. Bredas, M. Logdlund, W. R. Salaneck, *Nature* **1999**, *397*, 121-128.
[20] S. Pirouz, J. Duhamel, S. Jiang, A. Duggal, *Macromolecules* **2017**, *50*, 2467-2476.
[21] A. Rudnick, K.-J. Kass, E. Preis, U. Scherf, H. Bässler, A. Köhler, *J. Chem. Phys.* **2017**, *146*, 174903.
[22] H.-S. Jang, Y. Wang, Y. Lei, M.-P. Nieh, *J. Phys. Chem. C* **2013**, *117*, 1428-1435.
[23] a) X. Tian, Q. Zhang, M. Zhang, K. Uvdal, Q. Wang, J. Chen, W. Du, B. Huang, J. Wu, Y. Tian, *Chem. Sci.* **2017**, *8*, 142-149; b) Z. Mao, H. Jiang, Z. Li, C. Zhong, W. Zhang, Z. Liu, *Chem. Sci.* **2017**, *8*, 4533-4538.
[24] Y. Niko, H. Moritomo, H. Sugihara, Y. Suzuki, J. Kawamata, G.-i. Konishi, *J. Mater. Chem. B* **2015**, *3*, 184-190.
[25] M. Pawlicki, H. A. Collins, R. G. Denning, H. L. Anderson, *Angew. Chem. Int. Ed.* **2009**, *48*, 3244-3266.
[26] a) D. S. Corrêa, S. L. Oliveira, L. Misoguti, S. C. Zilio, R. F. Aroca, C. J. L. Constantino, C. R. Mendonça, *J. Phys. Chem. A* **2006**, *110*, 6433-6438; b) T. C. Barros, S. Brochsztain, V. G. Toscano, P. B. Filho, M. J. Politi, *J. Photochem. Photobiol. A: Chem.* **1997**, *111*, 97-104.
[27] H. Li, B. C. K. Tee, J. J. Cha, Y. Cui, J. W. Chung, S. Y. Lee, Z. Bao, *J. Am. Chem. Soc.* **2012**, *134*, 2760-2765.
[28] H. Li, C. Fan, M. Vosgueritchian, B. C. K. Tee, H. Chen, *J. Mater. Chem. C* **2014**, *2*, 3617-3624.

10.1002/anie.201707529

WILEY-VCH

COMMUNICATION

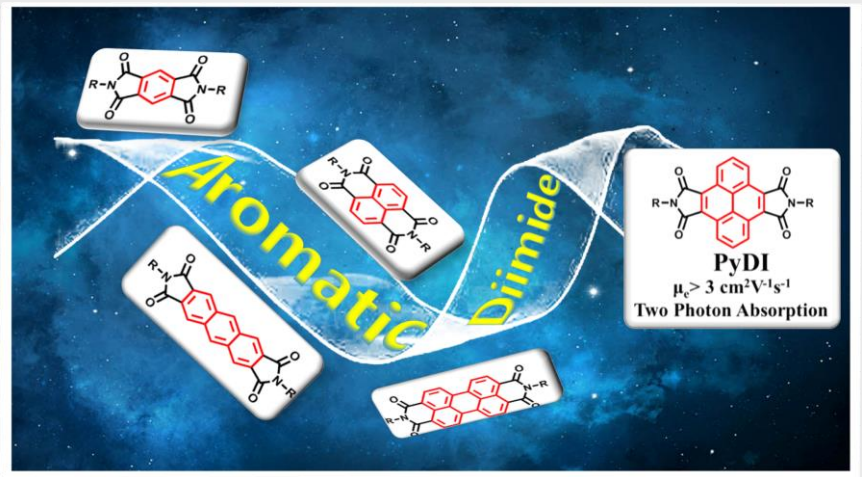

Ze-Hua Wu, Zhuo-Ting Huang, Rui-Xue Guo, Chun-Lin Sun, Li-Chuan Chen, Bing Sun, Zi-Fa Shi, Xiangfeng Shao, Hanying Li and Hao-Li Zhang**

Page No. – Page No.

4,5,9,10-Pyrene Diimides: A New Family of Aromatic Diimides Exhibiting High Electron Mobility and Two-Photon Excited Emission